www.nature.com/ismej

ISME

ARTICLE

Check for updates

Bacterial–fungal interactions promote parallel evolution of global transcriptional regulators in a widespread *Staphylococcus* species

Casey M. Cosetta[1,2], Brittany Niccum[1,2], Nick Kamkari[1], Michael Dente[1], Matthew Podniesinski[1] and Benjamin E. Wolfe[1]✉

Experimental studies of microbial evolution have largely focused on monocultures of model organisms, but most microbes live in communities where interactions with other species may impact rates and modes of evolution. Using the cheese rind model microbial community, we determined how species interactions shape the evolution of the widespread food- and animal-associated bacterium *Staphylococcus xylosus*. We evolved *S. xylosus* for 450 generations alone or in co-culture with one of three microbes: the yeast *Debaryomyces hansenii*, the bacterium *Brevibacterium aurantiacum*, and the mold *Penicillium solitum*. We used the frequency of colony morphology mutants (pigment and colony texture phenotypes) and whole-genome sequencing of isolates to quantify phenotypic and genomic evolution. The yeast *D. hansenii* strongly promoted diversification of *S. xylosus*. By the end of the experiment, all populations co-cultured with the yeast were dominated by pigment and colony morphology mutant phenotypes. Populations of *S. xylosus* grown alone, with *B. aurantiacum*, or with *P. solitum* did not evolve novel phenotypic diversity. Whole-genome sequencing of individual mutant isolates across all four treatments identified numerous unique mutations in the operons for the SigB, Agr, and WalRK global regulators, but only in the *D. hansenii* treatment. Phenotyping and RNA-seq experiments highlighted altered pigment and biofilm production, spreading, stress tolerance, and metabolism of *S. xylosus* mutants. Fitness experiments revealed antagonistic pleiotropy, where beneficial mutations that evolved in the presence of the yeast had strong negative fitness effects in other biotic environments. This work demonstrates that bacterial-fungal interactions can have long-term evolutionary consequences within multispecies microbiomes by facilitating the evolution of strain diversity.

The ISME Journal (2023) 17:1504–1516; https://doi.org/10.1038/s41396-023-01462-5

INTRODUCTION

Variation in ecological, genetic, physiological, and biochemical traits is commonly observed within microbial species. From metabolic heterogeneity in the bacterium *Escherichia coli* [1, 2] to divergent stress responses of the yeast *Saccharomyces cerevisiae* [3, 4], strain-level diversity is a fundamental feature of most microbes. Intraspecific variation can impact microbial ecology [5–7] and provides useful diversity to exploit for industrial purposes [4, 8, 9]. Despite its biological and economic significance, the mechanisms that generate intraspecific phenotypic variation within microbiomes are poorly characterized [10].

Adaptation to the challenges and opportunities presented by other microbial species may contribute to the generation of microbial strain diversity. Due to their large population sizes and fast generation times, microbes can rapidly adapt to a range of selective pressures [11–15]. Microbiologists have used experimental evolution to repeatedly subculture microbial species over many generations and monitor rapid adaptation to novel environments [11, 13, 16]. These experiments typically use monocultures of model species in the lab [17–19], but most microbes in nature live in multispecies communities where they experience strong selective pressures from other microbes [20–25]. Because interspecific microbial interactions have been largely excluded from experimental evolution, our understanding of the dynamics and mechanisms of microbial adaptation in multispecies microbiomes is incomplete and lacking biotic context.

Based on examples from macroorganisms and some preliminary studies in synthetic microbial systems, microbe-microbe interactions can mediate adaptation by reducing population size and subsequent rates of mutations [26], inducing shifts to alternative niches via competition [27, 28], producing novel niches via resource provisioning [29, 30], or by inducing or releasing environmental stresses and impacting selection on stress and defense systems [31]. This is not an exhaustive set of all potential mechanisms underlying microbial adaptation to biotic environments and multiple mechanisms may be operating in the presence of a single neighbor.

A few highly synthetic studies of laboratory isolates have started to identify different mechanisms of microbial adaptation to varying biotic environments [28, 30, 32–37]. These studies begin to add biological complexity to microbial evolution, but they rarely attempt to explain adaptation of microbial populations in naturally occurring communities where ecological environments of ancestral and evolved strains can be clearly defined. These studies also often use selective environments that may not be

[1]Department of Biology, Tufts University, Medford, MA 02155, USA. [2]These authors contributed equally: Casey Cosetta, Brittany Niccum. ✉email: benjamin.wolfe@tufts.edu

Received: 9 February 2023 Revised: 6 June 2023 Accepted: 15 June 2023
Published online: 31 July 2023

relevant to the interactions that microbes experience in naturally forming microbial systems. Moreover, this work has been limited to a few target species (mainly *Pseudomonas fluorescens*) and does not usually identify specific mechanisms underlying microbial adaptation to novel biotic environments [33].

The domestication of wild microbes in fermented food environments provides a unique opportunity to fill major gaps in our understanding of how interspecific interactions impact microbial adaptation. In some fermented foods - such as sourdough, kimchi, and certain cheeses - wild microbial species colonize the food substrate and become part of the food microbiome [38–43]. As continuous batches of food are made in the same location, recirculating microbial populations can adapt to novel abiotic and biotic environments [43, 44]. Hints of adaptive evolution come from comparative studies of domesticated and wild microbes [44–46]. But the mechanisms that drive the adaptation of fermented food microbes are unknown due to a limited number of studies experimentally recreating the domestication process [43, 44, 47].

In this work, we use one bacterium that is widespread in cheese rinds - *Staphylococcus xylosus* - as a target species for evolution in different biotic environments. This *Staphylococcus* species is often used as a starter culture in the production of cheese and fermented meats [48], but can also be found associated with various mammals [49]. This bacterium is an early colonizer of cheese rinds and interacts with a range of fungal and bacterial species during cheese rind succession ([50], Fig. 1A). We have observed considerable variation in colony morphology and pigmentation of strains isolated from cheese and other fermented food environments (Fig. 1B). The evolutionary processes that shape this remarkable phenotypic diversity in *S. xylosus* have not been characterized.

To determine if microbial interactions contribute to the phenotypic and genomic diversification of *S. xylosus*, we evolved an isolate of this bacterium (strain BC10) either alone or co-cultured with each of three different cheese rind neighbor species. We predicted that microbe-microbe interactions might promote diversification in the presence of some neighboring species that provide novel ecological opportunities and inhibit diversification in the presence of other species that are strong competitors. Because the evolution of colony morphology often correlates with clear underlying adaptive mutations in *Staphylococcus* species [51, 52], we were able to track phenotypic diversity of colonies over time as a proxy for diversification under the different biotic conditions. We also conducted whole-genome sequencing of evolved isolates from the end of the experiment to measure genomic diversity and determine mutations that were driving phenotypic diversity. Competition experiments, phenotypic assays, and RNA sequencing of select isolates revealed underlying mechanisms of adaptation and intriguing trade-offs associated with the adaptation of *S. xylosus* to different biotic environments.

RESULTS

The yeast *Debaryomyces hansenii* promotes phenotypic evolution of *S. xylosus*

We serially transferred populations of *S. xylosus* grown in four different biotic environments: (1) without a neighbor (hereafter Alone), (2) with the bacterium *Brevibacterium aurantiacum* (hereafter +*Brevibacterium*), (3) with the yeast *Debaryomyces hansenii* (hereafter +*Debaryomyces*), and (4) with the filamentous fungus *Penicillium solitum* (hereafter +*Penicillium*). All of these microbes were isolated from the same natural rind cheese that has been the focus of previous research in this model system, and span a range of life history strategies and temporal dynamics in community succession [50, 53–55]. Both *S. xylosus* species and yeasts such as *D. hansenii* are abundant in early stages of cheese rind development, while *Penicillium* molds and Actinobacteria such as *Brevibacterium* species thrive in the later stages of rind development [50, 54]. Because representatives of all three neighboring taxa have been shown to both inhibit or promote the growth of *S. xylosus* and other *Staphylococcus* species [50, 54], we predicted that the different biotic environments created by these neighbors would impact phenotypic and genomic evolution of *S. xylosus*.

Ten replicate populations of *S. xylosus* in each of the four different conditions were transferred weekly for 16 weeks (about 450 generations). At each transfer, populations were plated out to determine the number of wild-type and mutant colonies and to determine the presence of the interacting neighbor species. We did not attempt to distinguish different types of mutant colony morphologies within populations because some of these differences are subtle and difficult to track over time. We simply tracked the proportion of total mutant (not wild-type/ancestor) colonies over time as an approximation of phenotypic evolution within the *S. xylosus* populations. We acknowledge that this approach misses some important dynamics of strain evolution over time and will not capture genomic diversification that does not cause colony morphology changes. But it is a useful tool to track phenotypic diversification that also pointed to some fascinating patterns of genomic evolution at the end of the experiment.

Five weeks into the experiment, we noticed that many colonies across replicate +*Debaryomyces* populations had morphotypes that were different in appearance compared to the ancestor (Fig. 1D). These colonies were often reduced in pigmentation, were not as wrinkly, and often had a shiny appearance that was not apparent in the ancestor (Fig. 1E). By the end of the experiment, most of the +*Debaryomyces* replicate populations were taken over by mutant colony phenotypes (99% mean phenotypic mutant frequency across populations; Fig. 1D). In contrast to the +*Debaryomyces* treatment, very few phenotypic mutant colony phenotypes were observed in the Alone (0.02% frequency), +*Brevibacterium* (0% frequency), or +*Penicillium* (0% frequency) treatments. There were fluctuations at certain transfer points in phenotypic mutant frequencies in these other treatments (sometimes up to nearly 20%), but only in the +*Debaryomyces* treatment did phenotypic mutant frequencies stabilize at or nearly 100% frequency. Interacting neighbor species were maintained throughout the 16 weeks of the experiment (Fig. S1).

Differences in population sizes caused by both abiotic and biotic factors can impact rates of evolution [26, 56] and may explain the differences in phenotypic evolution across the four treatments. For example, biotic interactions that suppress population size may inhibit evolution [57, 58]. There were significant differences in population size over time across the four treatments, with the +*Penicillium* treatment having the highest mean population size (ANOVA $F_{3,38} = 58.2$; $p < 0.001$). However, the +*Debaryomyces* populations where we observed the high phenotypic mutant frequency were not significantly different in population size from the Alone or +*Penicillium* treatments with low phenotypic mutant frequencies (Fig. S2), suggesting that population size does not explain the vastly different amounts of phenotypic evolution we observed.

Mutations in global regulatory genes explain *S. xylosus* phenotypic evolution with *Debaryomyces hansenii*

To better understand genomic changes that drove the phenotypic diversification of *S. xylosus*, we randomly selected seven colonies from three representative populations from each of the four treatments for whole-genome sequencing. We mapped Illumina sequence reads from each of these evolved isolates to the *S. xylosus* reference genome to identify SNPs and other genomic changes in each evolved isolate. Corroborating the phenotypic evolution observed in the +*Debaryomyces* treatment, we observed a higher frequency of non-synonymous mutations in isolates from that treatment (ANOVA $F_{3,11} = 6.4$, $p < 0.05$; Fig. 2A).

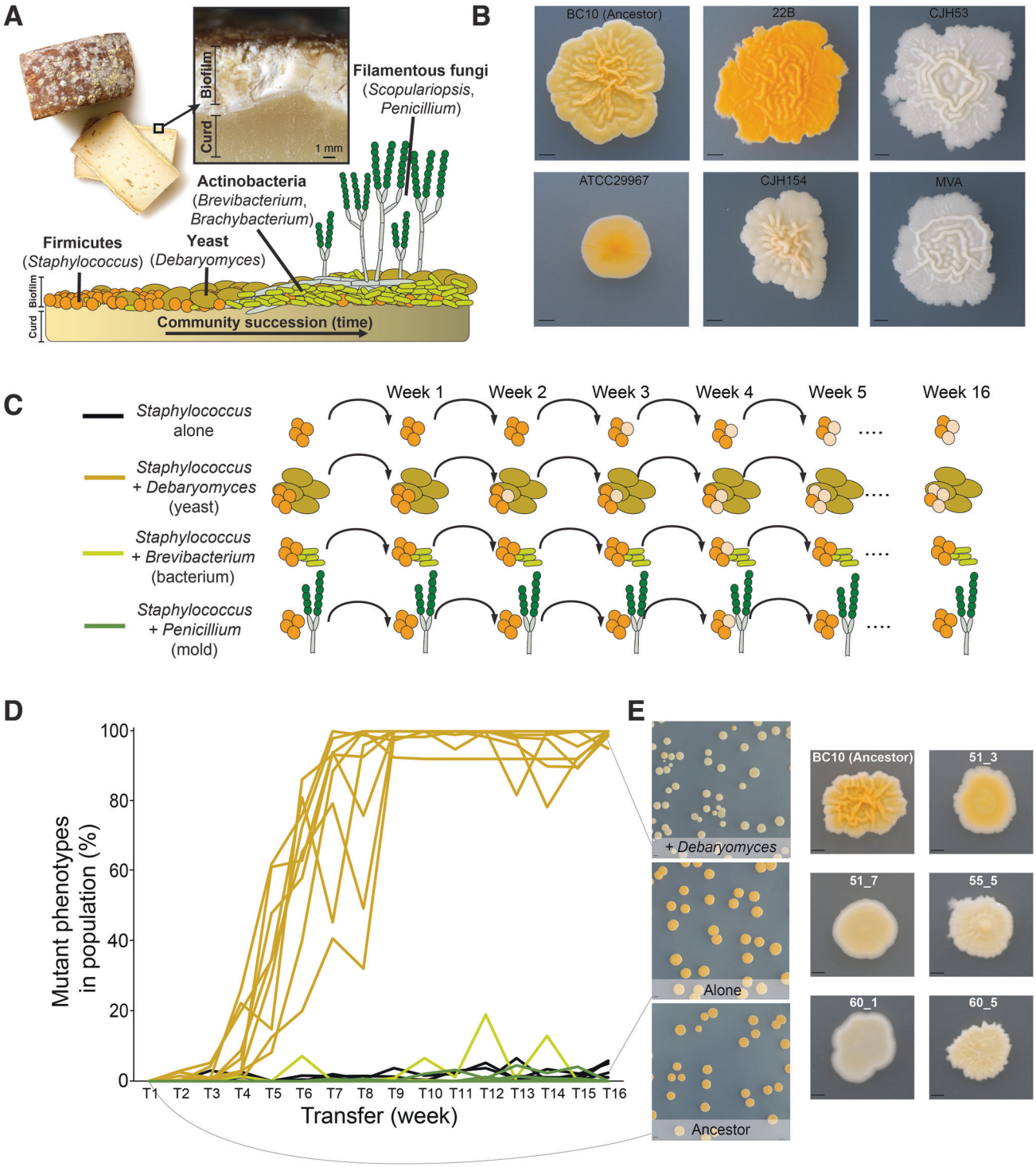

Fig. 1 The yeast *Debaryomyces hansenii* causes phenotypic diversification of *S. xylosus* BC10 during experimental evolution. A Overview of the cheese rind microbiome and the microbial species used in this manuscript including *Staphylococcus xylosus*, *Debaryomyces hansenii*, *Brevibacterium aurantiacum*, and *Penicillium solitum*. **B** Phenotypic variation across different isolates of *Staphylococcus xylosus*. All isolates are from cheese except for ATCC29967, the reference isolate for the species. BC10 is the strain used in this study. The scale bar represents 2.5 mm. **C** Overview of the experimental design used for the evolution study. **D** Frequency of phenotypic mutants in replicate populations across the four experimental treatments. Line colors correspond with the treatments indicated in C. Each line represents a replicate population, with ten replicates per treatment. One +*Debaryomyces* replicate became contaminated and had to be removed from the experiment. Mutant frequency was significantly higher in the +*Debaryomyces* treatment compared to the other three treatments at the final transfer (Kruskal–Wallis $p < 0.0001$, with Mann–Whitney post-hoc tests). **E** Examples of typical colony morphotypes within a population of Ancestor (the wild-type BC10), a population evolved Alone (without another microbial species), and a population in the +*Debaryomyces* treatment. Note the distinct difference in color in +*Debaryomyces* compared to the other two populations. More detailed examples of colony morphologies are shown on the right. 51_3, 51_7, 55_5, 60_1, and 60_5 were used for additional experiments in Figs. 3–5. The scale bar in the population photos on the left represents 5 mm and the scale bar in the closeup photos represents 1 mm.

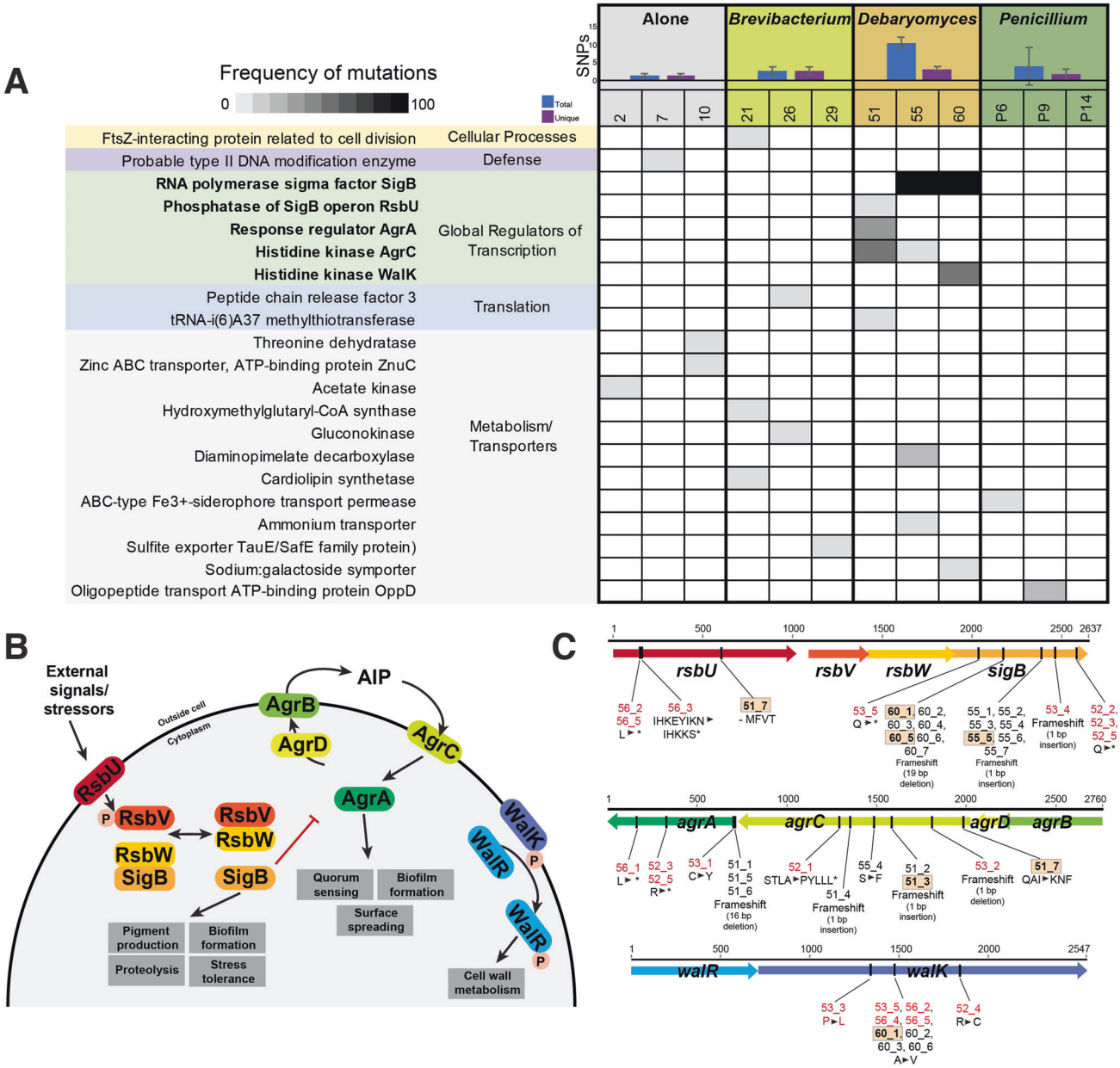

Fig. 2 Whole-genome sequencing identifies mutations in putative global regulators of *S. xylosus* BC10 in the +*Debaryomyces* treatment. **A** Blue and purple bar graphs show number of SNPs (total in blue, number across unique genes in purple) detected across *S. xylosus* from three populations within each of the four biotic treatments (Alone, +*Brevibacterium*, +*Debaryomyces*, and +*Penicillium*). Shaded cells show frequency of non-synonymous mutations within a gene within a population (columns) based on sequencing 7 isolates per population. Only genes with a putative function assigned are shown. See Fig. S3 for a full table of all mutations, including those with unknown functions and those in the additional +*Debaryomyces* treatments that were sequenced. Numbers 1–10, 21–30, 51–60, and 61–70 are used to indicate unique populations. There were other experimental populations included in the initial experiment (31–40, 41–50), but they are excluded from this manuscript because the neighbor treatment went extinct. **B** Overview of the components of the three global regulatory systems where many mutations were detected in the +*Debaryomyces* treatment. These systems are poorly characterized in *S. xylosus*, so the potential structure and function of these systems is inferred from what is known in *S. aureus*. **C** Location and type of mutations observed in the *sigB*, *agr*, and *walRK* loci. Strains indicated in red font were from the additional +*Debaryomyces* treatments that were sequenced and are not included in (**A**), but are found in Fig. S3.

All isolates from the +*Debaryomyces* treatment contained at least one non-synonymous mutation, whereas fewer than half of the isolates from the other treatments had a non-synonymous mutation. One intergenic and seven synonymous mutations were observed across the sequenced isolates (Table S1).

When considering the types of genes with mutations across all treatments, a very distinct pattern emerged: all isolates from the +*Debaryomyces* treatment had at least one mutation in a global regulator of transcription, including the alternative sigma factor B (SigB), the accessory gene regulator (Agr), and the WalRK system (Fig. 2A). As discussed below, all three of these systems regulate key cellular processes, including biofilm and pigment formation, and could explain the increase of novel colony morphotypes in the +*Debaryomyces* treatment. We did not detect mutations in global regulators of transcription in any of the other treatments. Mutations in genes related to metabolism and nutrient transport,

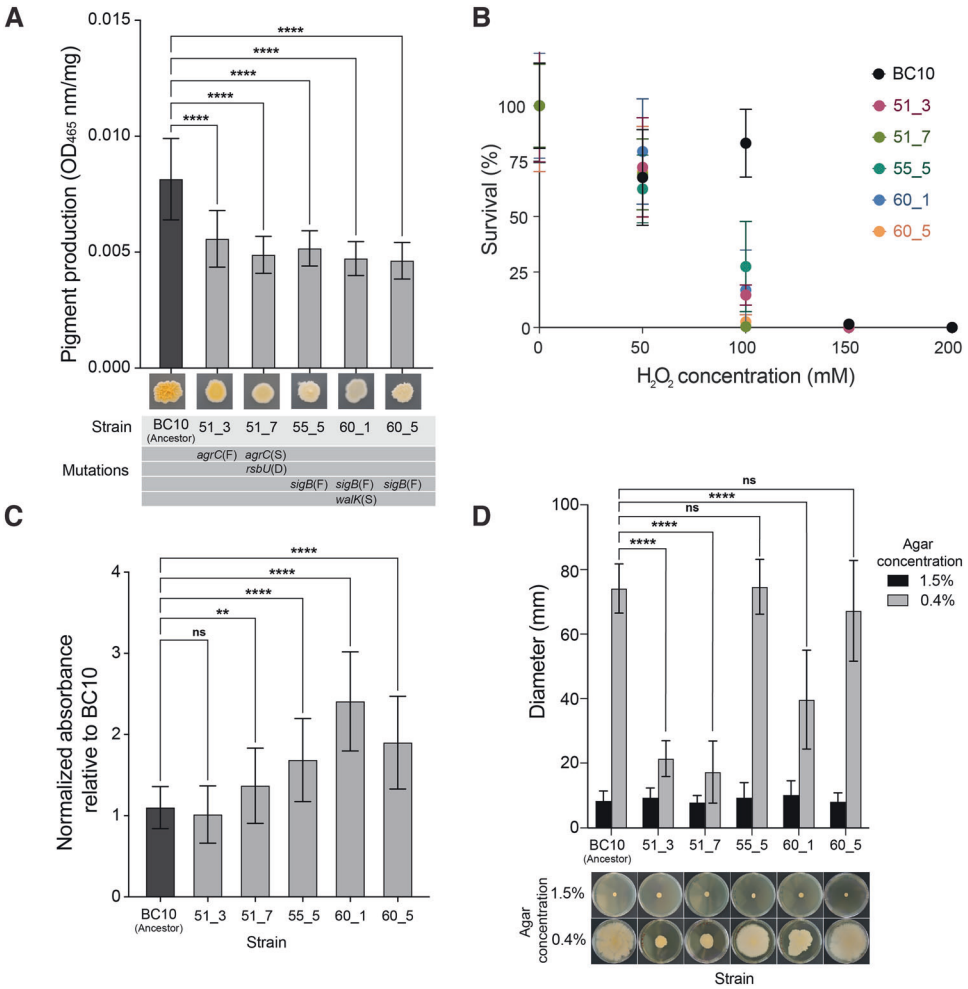

Fig. 3 Phenotypic assays reveal biological impacts of global regulator mutations in evolved *S. xylosus* BC10. A Pigment production in the ancestor and evolved strains of *S. xylosus* BC10. Bars represent means and error bars represent standard deviations. **** indicates $p < 0.0001$ based on ANOVA with Dunnett's test. Data are from three independent experiments with six replicates of each treatment within each experiment. **B** Survival of the ancestor and evolved strains of *S. xylosus* BC10 across a range of H_2O_2 concentrations. Dots represent means and error bars represent standard deviations. At 100 mM, the *S. xylosus* BC10 ancestor had a higher survival compared to all evolved strains (two-way ANOVA, $p < 0.0001$). Data are from two independent experiments with eight replicates of each treatment within each experiment. **C** Biofilm production of ancestor and evolved strains of *S. xylosus* BC10. Bars represent means and error bars represent standard deviations. ** indicates $p < 0.01$ and **** indicates $p < 0.0001$ based on ANOVA with Dunnett's test. ns indicates not significant. Data are from three independent experiments with nine replicates of each treatment within each experiment. **D** Spreading of ancestor and evolved strains of *S. xylosus* BC10. Photos at the bottom of the graph show representative plates from the 1.5% (low spreading) and 0.4% (high spreading) conditions. Bars represent means and error bars represent standard deviations. **** indicates $p < 0.0001$ based on ANOVA with Dunnett's test. ns indicates not significant. Data are from three independent experiments with five replicates of each treatment within each experiment.

translation, defense, and other cellular processes occurred across all four treatments, but there was not a specific enrichment of these mutations in any treatment (Fig. 2A). To confirm that this pattern of mutations in global regulators was consistent beyond the three +*Debaryomyces* populations that we sampled (51, 55, 60), we sequenced genomes of 5 isolates from an additional three populations (52, 53, 56) from the +*Debaryomyces* treatment and found an identical pattern of mutations in global regulators of transcription across all three populations (Fig. S3).

SigB is very well-characterized in *Staphylococcus aureus* and other Gram-positive bacterial species, where it has been shown to regulate the expression of hundreds of genes [59–61] (Fig. 2B). The *sigB* operon includes the genes *sigB*, *rsbU*, *rsbV*, and *rsbW* (Fig. 2C). A diverse set of mutations in the sigB operon were detected across populations, with most mutations observed in *sigB*, a few in *rsbU*, and no mutations in *rsbV* or *rsbW* (Fig. 2C). Mutations in *sigB* ranged from amino acid substitutions to both small (1 bp insertion) and large (19 bp deletion) frameshift mutations. Some populations contained the same mutation across all isolates (e.g. a major deletion of 19 base pairs in all isolates from population 60; Fig. 2C) whereas other populations had multiple strains with unique *sigB* mutations (e.g. a predicted truncation in 53_5 and a 1 bp insertion causing a frameshift in 53_4). Three different mutations were detected in *rsbU*: a 12 base-pair deletion causing a predicted loss of 4 amino acids in an isolate from population 51 (strain 51_7, Fig. 2C), a predicted truncation in two isolates from population 56, and amino acid substitutions and a truncation in another isolate from population 56.

Agr is a quorum sensing regulator that has been well-characterized in *S. aureus* and other *Staphylococcus* species [62–64] (Fig. 2B). The *agr* operon consists of *agrA* and *agr*C (encoding a two-component signal transduction system), *agrD* (encoding a propeptide that becomes the quorum sensing molecule), and *agrB* (encoding a transmembrane protein). Consistent with patterns of Agr evolution in *S. aureus* [63], all mutations we observed were in *agrA* and *agrC* (Fig. 2C). Most

mutations were observed in population 51, with four unique mutations distributed across the 7 isolates, including both large deletions (in *agrA*) and small insertions/deletions (in *agrC*) causing frameshifts (Fig. 2C). An amino acid substitution was observed in one isolate from population 55. Additional *agrA* and *agrC* mutations were observed in the additional +*Debaryomyces* populations that were sequenced (Figs. 2C and S3).

The *walRK* operon (sometimes referred to as *walKR*, *yycGF*, or *vicKR*) is another regulatory region where multiple mutations were observed in +*Debaryomyces* isolates. WalRK is a two-component system that controls a variety of processes in *S. aureus*, including cell wall metabolism [65] (Fig. 2B). Although the functions of WalRK have not been characterized in *S. xylosus*, previous work in *S. aureus* has demonstrated that single mutations in *walK* or *walR* can impact drug resistance and cell wall structure [66]. Three different amino acid substitutions were observed in the predicted *walK* gene, including one mutation that occurred across three different populations (53, 56, and 60; Fig. 2C). Some strains had mutations in both the *walK* and either *rsbU* (strains 56_2, 56_5) or *sigB* (strains 53_5, 60_1, 60_2, 60_3, 60_6).

Collectively, our resequencing of evolved mutants highlights parallel mutations in global regulators across replicate +*Debaryomyces* populations. The regulatory systems noted above have not been characterized in *S. xylosus*, so we cannot know for sure that they regulate the same genes and traits as in *S. aureus* where they have been well-studied. But many components of these systems are conserved across *Staphylococcus* species or Gram-positive bacteria more generally [67–69], and may operate in a similar manner in *S. xylosus*.

S. xylosus mutants have altered pigment, biofilm, and stress tolerance phenotypes

Because whole-genome sequence data identified mutations in global regulators known to control phenotypes in *Staphylococcus* species, we used a series of assays to characterize these traits in a subset of evolved strains of *S. xylosus* BC10. Our goal with these assays was to better understand how the mutations impacted the biology of *S. xylosus* and whether the mutations in the global regulators had similar effects in *S. xylosus* as they do in other *Staphylococcus* species. We selected mutants from different replicate populations of the +*Debaryomyces* treatment that spanned a range of genes and different mutations within those genes (strains 51_3, 51_7, 55_5, 60_1, and 60_5). These mutants did not have other mutations in predicted coding regions, so changes in phenotypes observed in these strains could be attributed to mutations in the global regulators.

Colonies of *S. xylosus* evolved in the +*Debaryomyces* treatment had noticeably lighter colonies compared to other populations (Fig. 3A). We predicted that these differences could be due to changes in production of the carotenoid staphyloxanthin. This pigment gives *S. aureus* and other *Staphylococcus* species a golden or orange appearance and is encoded by the *crtOPQMN* operon that is controlled by SigB [70]. Mutations in the SigB operon can lead to reduced pigmentation [52, 71]. Colorimetric assays indicated that the ancestor produced significantly more staphyloxanthin pigment compared to all other evolved strains (one-way ANOVA; $p < 0.001$). The strains containing a mutation in the *sigB* system produced the least amount of pigment, with strain 60_5 only producing 43% compared to the ancestor. Strains 51_3 and 51_7 also produced significantly less pigment, 68 and 60% compared to the ancestor, respectively.

Because carotenoids like staphyloxanthin can function as antioxidants in *Staphylococcus* species [72, 73] and may play a role in how *S. xylosus* interacts with the cheese rind environment, we next tested tolerance of the *S. xylosus* strains to oxidative stress in the form of hydrogen peroxide. All strains were equally susceptible to 50 mM of H_2O_2, but the ancestor BC10 had a higher tolerance to 100 mM than the evolved strains (Fig. 3B). At 150 mM, there were no viable cells in any population. These data suggest that *S. xylosus* carotenoid levels can provide similar oxidative protection as in *S. aureus* and other *Staphylococcus* species.

Biofilm formation is a key ecological trait that determines how microbes interact with both abiotic and biotic elements of their environment [74–76]. To understand if the observed mutations in the evolved *S. xylosus* affected biofilm production, we used a crystal violet staining assay to quantify biofilm production. In previous studies of *S. aureus*, expression of *sigB* has been linked with the ability to produce biofilms and mutations in *sigB* have resulted in biofilm-negative phenotypes [77, 78]. Mutations in the *agr* system can cause increased biofilm production in *S. aureus* because a functional *agr* inhibits biofilm production [79]. Based on this, we predicted that *S. xylosus* strains that had mutations in *sigB* would result in decreased biofilm formation compared to the ancestor, while the strains with *agr* mutations would have increased or similar levels of production. In contrast to these predictions, strains 55_5, 60_1, and 60_5 (all with *sigB* frameshift mutations) produced significantly more biofilm at 1.53, 2.18, and 1.78 times more than the BC10 ancestor (Fig. 3C). Aligning with our predictions, the two strains that had *agrC* mutations (51_3 and 51_7) had increased or equal biofilm formation compared to the ancestor (1.2 times more for 51_7 produced and equal production for 51_3, Fig. 3C).

The ability to spread across surfaces is an important trait for the virulence of *S. aureus* [80, 81], and may also be important for how *S. xylosus* spreads across cheese surfaces [82, 83]. Previous studies have shown that the *agr* system is involved in the production of a biosurfactant that allows *Staphylococcus* species to spread, and that disruption of the *agr* system can cause reduced spreading [51, 52, 84]. Both *agr* mutants were found to be deficient in colony spreading; strain 51_3 and 51_7 had a 71.1% and 76.7% reduction in spreading compared to the BC10 ancestor, respectively (Fig. 3D). Strain 60_1 had an average of 46.5% reduction in spreading with irregular colony edges (Fig. 3D). Strains 55_5 and 60_5 were not statistically different from the ancestor (Fig. 3D).

These targeted phenotypic data demonstrate that *S. xylosus* mutations that evolved in the presence of *D. hansenii* can have major impacts on the biology of this bacterium. Our data also suggest that some of the functions of these global regulators from *S. aureus* may be conserved in *S. xylosus*; predictions about how mutations in the global regulators might alter phenotypes based on *S. aureus* biology were often correct.

RNA-seq reveals decreased expression of key metabolic pathways in evolved *S. xylosus* strains

To better understand other underlying changes in the biology of the evolved strains that were not captured with the phenotypic assays, we used RNA-seq to quantify global transcriptional differences between the ancestor BC10 and three mutants: 51_3, 55_5, and 60_1. We selected these three strains for RNA-seq because they ranged in *sigB*, *agr*, and *walRK* mutations and had no or few other genetic changes in other regions of their genome. We compared global gene expression at 3 days of growth on cheese curd agar because the bacterium is in late exponential phase and RNA can be easily extracted at this time point.

Each of the three evolved strains had major shifts in global transcription compared to the ancestor BC10 (Fig. 4A–C; Tables S2–S5). With a differentially expressed gene (DEG) cutoff of a $\log_2$ ratio of 1/−1 and a false discovery rate (FDR) corrected p value of 0.05, many genes across the genome of the bacterium had lower expression levels in the mutants: 23% of predicted genes across the genome in 51_3, 13% in 55_5, and 22% in 60_1. A lower, but still substantial number of genes were also upregulated across the three strains: 18% of genes in 51_3, 7% in 55_5, and 16% in 60_1. These broad patterns of DEGs support previous studies showing that SigB, Agr, and WalRK can have broad transcriptional control in *Staphylococcus* species and that mutations in these global regulators can alter transcriptional networks within these species [52, 85–89].

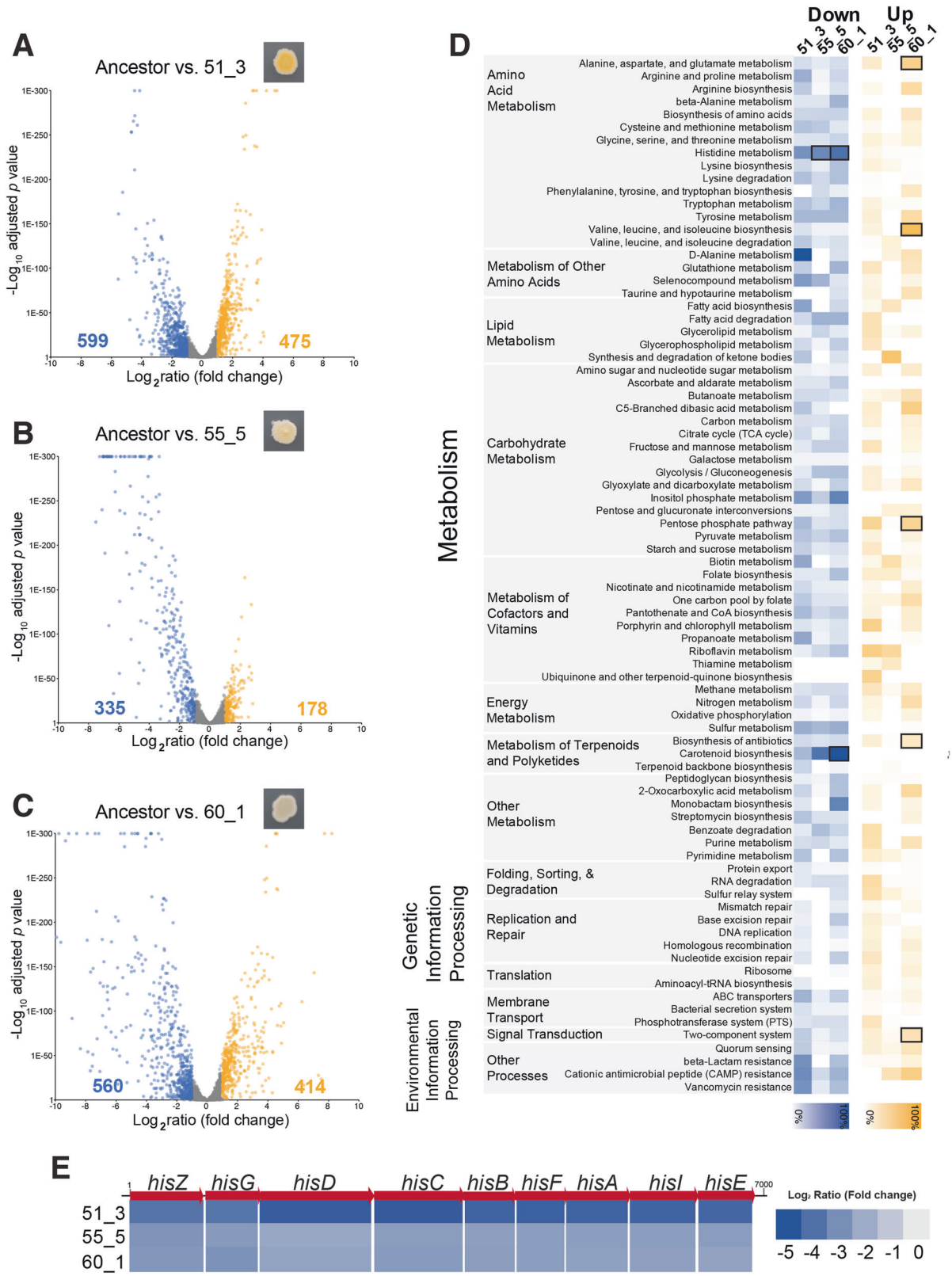

Fig. 4 RNA sequencing highlights transcriptomic impacts of global regulator mutations in *S. xylosus* BC10. Volcano plots showing changes in gene expression in mutant strain 51_3 (**A**), 55_5 (**B**), and 60_1 (**C**) compared to the ancestor BC10. Each dot represents a gene in the BC10 genome. Yellow dots are genes with significant increases in expression in the mutants. Blue dots are genes with significant decreases in expression compared to the ancestor. Numbers on the left and right of the x-axes indicate the number of genes that were significantly higher (yellow) or lower (blue) in expression for each mutant. **D** KOBAS pathway analysis of differentially expressed genes for each mutant. Blue or yellow shading indicates percent of genes in a pathway that were differentially expressed. Bold boxes indicate significant enrichment of a pathway based on a Fisher's exact test with FDR correction. **E** Fold-change in expression of the nine genes in the *his* operon for histidine biosynthesis.

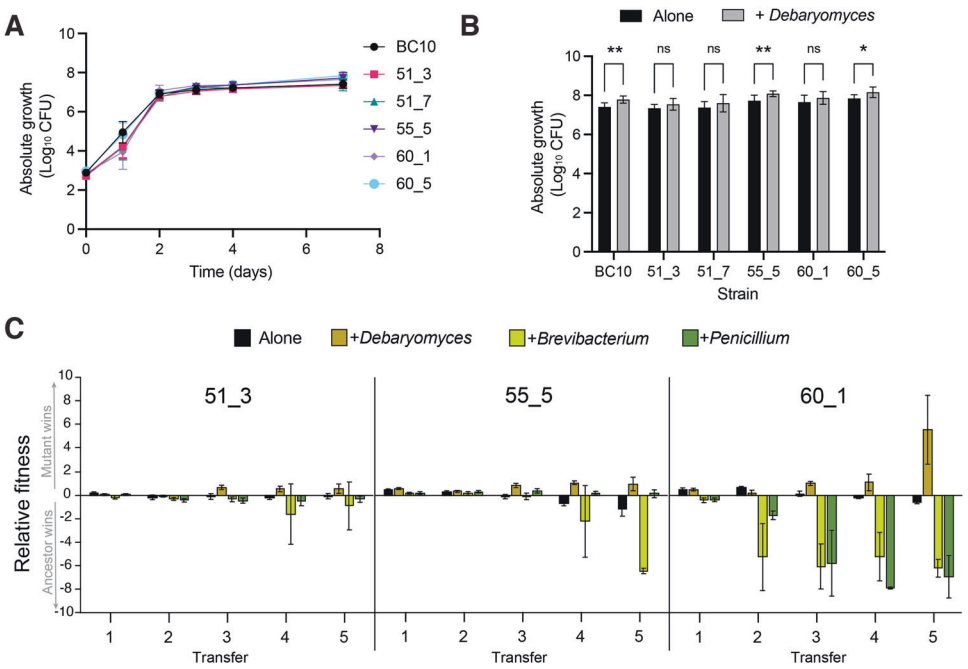

Fig. 5 Growth and competition experiments reveal fitness of evolved *S. xylosus* mutants in different biotic environments. A Growth of ancestor and evolved strains on cheese curd agar alone. Data represent mean CFUs at each time point and error bars are standard errors of the mean. Data are from three independent experiments with five replicates of each treatment within each experiment. **B** Growth of ancestor and evolved strains on cheese curd agar with and without the yeast *D. hansenii* after 7 days of growth. Data represent mean CFUs and error bars are one standard error of the mean. Data are from three independent experiments with five replicates of each treatment within each experiment. *D. hansenii* increased the growth of the isolates compared to growth alone ($F_{5,161} = 3.4$; $p < 0.001$). For post-hoc comparisons, ** = $p < 0.005$; * = $p < 0.05$. **C** Fitness of ancestor and mutant strains of *S. xylosus* when competed in initially identical ratios in different biotic environments. The ancestor:mutant mix was grown in four treatments and passaged five times to mimic the repeated cycles of growth in the evolution experiment. Relative fitness is expressed as $\log_{10}((\text{CFUs of mutant strain} + 1) \div (\text{CFUs of ancestor strain} + 1))$. A positive relative fitness means that the mutant strain reached a higher proportion of the total number of CFUs when competing with the ancestor. A negative fitness means the ancestor strain reached a higher proportion. Error bars represent one standard deviation of the mean with eight replicates of each treatment.

Across the three mutants, most of the differentially expressed genes were associated with metabolism, including the biosynthesis and degradation of amino acids, lipids, carbohydrates, and secondary metabolites (Fig. 4D; Tables S6–S9). When we used pathway enrichment analysis to identify what DEGs were significantly associated with all three mutants, two patterns of decreased pathway expression emerged. One pattern involves the production of carotenoids. Most of the genes in the staphyloxanthin biosynthesis operon were downregulated in all three mutants compared to the ancestor (Fig. 4D). This was especially pronounced in strains 55_5 and 60_1 and corroborates our observations and pigment assays above where 55_5 and 60_1 were much lighter in color compared to the ancestor. This also aligns with previous studies demonstrating that disruption of normal SigB functioning can alter pigment production in *S. aureus* [52].

The other strong pattern of decreased pathway expression across all three mutants was histidine metabolism (Fig. 4D). Specifically, all genes in a putative histidine biosynthesis operon were strongly downregulated in all three mutants compared to the ancestor (Fig. 4E). In a previous study of another *S. xylosus* strain, this histidine operon was upregulated in growth in a dairy matrix due to the low availability of histidine and other free amino acids [90]. Downregulation of histidine biosynthesis and other amino acid metabolism in the evolved *S. xylosus* BC10 mutants suggests a parallel shift in nutrient requirements in all three strains, despite different mutations that caused the downregulation.

Competition experiments reveal fitness trade-offs of evolved *S. xylosus* strains in different biotic environments

To better understand how the mutations and altered phenotypes observed above impact the fitness of evolved *S. xylosus* BC10 strains, we conducted a series of assays to measure growth and competitive abilities of all strains in different biotic environments. First, we measured the growth of the ancestor and evolved strains growing individually on cheese curd agar for 7 days. All strains demonstrated typical growth curves on cheese, reaching stationary phase around 3 days of growth. There were significant differences in growth over time across all strains ($F_{5,84} = 6.9$, $p < 0.001$; Table S10), which was driven by two major patterns. First, early in growth at day 1, all strains except 60_5 had lower growth compared to the ancestor (Fig. 5A), suggesting a lag in log phase for most mutant strains. Second, at the final time point of 7 days, two strains (55_5, 60_6) had significantly higher abundance compared to the ancestor (Fig. 5A). These data demonstrate that the genomic changes in the evolved strains had minor and inconsistent effects on their growth compared to the ancestor.

Given the high frequency of global regulator mutations in the +*Debaryomyces* treatment, we next tested how the presence of *D. hansenii* impacted the growth of each of the ancestor and evolved strains. We predicted that *D. hansenii* may increase the growth of evolved strains relative to the ancestor because they should have a fitness benefit from living with the yeast. Surprisingly, all strains were slightly stimulated by the presence of *D. hansenii*, with significant increases in growth observed for the Ancestor, 55_5, and 60_5 (Fig. 5B).

Growth as single isolates does not fully capture mutant fitness in competitive environments; evolved strains need to compete with ancestor strains during evolution to become dominant lineages at the end of the experiment. Additionally, very small fitness differences that could accumulate to have major impacts over time may not be apparent in the short time scales used in the

previous experiments. Therefore, we next conducted fitness experiments where we grew each evolved strain in a 50:50 ratio with the ancestor BC10 strain. Because the evolved strains had unique colony morphologies, we were able to directly compete the strains and distinguish them on output plates. The ancestor:mutant pairing was grown either alone (without any other neighboring microbes) or in the presence of the biotic treatments used in the evolution experiment (+*Debaryomyces*, +*Brevibacterium*, and +*Penicillium*). We transferred the competition experiments five times after 7 days of growth to mimic the passaging that occurred in the original evolution experiment. We predicted that evolved strains would have a higher fitness relative to ancestor strains in the +*Debaryomyces* given how they dominated those populations in the evolution experiment. We only did these experiments with the three strains used in the RNA-seq analysis (51_3, 55_5, and 60_1) because they spanned the range of phenotypes and mutations observed in the evolution experiment.

As predicted, strains 51_3, 55_5, and 60_1 all had a significantly higher relative fitness in the +*Debaryomyces* treatment after multiple rounds of passaging (ANOVA 51_3 $F_{3,29} = 7.9$, $p < 0.001$; 55_5 $F_{3,29} = 8.5$ $p < 0.001$; 60_1 $F_{3,29} = 10.2$ $p < 0.001$; Fig. 5C). In the Alone treatment with no neighbors, all evolved strains had slight negative fitness compared to the ancestor, which corroborates the lack of these mutants in the Alone evolution populations. We repeated this experiment again with the Alone and +*Debaryomyces* treatment and observed the same pattern of increased fitness of the evolved strains in the +*Debaryomyces* treatment and lower fitness in the Alone treatment (Fig. S4).

Some evolved strains had strong fitness defects in other biotic environments, especially 60_1 in the +*Brevibacterium* and +*Penicillium* environments (Fig. 5C). This suggests that the altered SigB, Agr, and WalRK regulation in these evolved strains impairs their growth relative to the ancestor strain and explains why they did not evolve in the Alone, +*Brevibacterium*, or +*Penicillium* treatments. We do not know the exact impact of the mutations on WalRK functions in 60_1, but this regulator is known to play key roles in cell wall metabolism [89], so altered functions of WalRK may make evolved strains unable to grow well in the presence of +*Brevibacterium* or +*Penicillium*. The severe fitness trade-offs observed for the evolved strains in different biotic environments is an example of antagonistic pleiotropy [91], where beneficial mutations in the presence of the yeast *D. hansenii* can have strong negative fitness effects in other biotic environments.

DISCUSSION

One major theme from this work is that interspecific microbe-microbe interactions can shape the evolutionary trajectories of bacteria. While in the Alone, +*Brevibacterium*, and +*Penicillium* treatments we did not see considerable phenotypic evolution or consistent mutations in populations, the yeast *D. hansenii* promoted genomic and phenotypic diversification of *S. xylosus*. In a short period of time, many different mutant colony types emerged that were distinct from the ancestral colony morphology, with unique pigmentation and colony structure. This pattern emerged across replicate populations and involved distinct mutations in the same global regulator loci, providing strong evidence of parallel adaptation in this biotic environment.

There are several key nuances and limitations of our work that should be considered when contextualizing it within the cheese rind microbiome and other microbial systems. First, we did not attempt to prevent or control the evolution of the neighbors in our experiment, so the selection pressures experienced by *S. xylosus* throughout time may have shifted if ecologically relevant traits of the neighbors evolved. This was a conscious decision as we were trying to mimic population dynamics in cheese aging facilities where both target microbes and neighboring microbes might evolve. We did not observe any obvious growth or colony morphology changes in the neighbors and previous research in our lab has demonstrated that one neighbor (*Penicillium*) does not evolve new phenotypes if bacteria are present [47]. Second, our studies were confined to a controlled laboratory environment, so we do not know how often mutants we have observed here would evolve in cheese production and aging environments. However, we believe there is considerable potential for similar evolutionary processes to unfold in cheese aging facilities. In these environments, *S. xylosus* populations experience varying biotic environments due to patchiness of cheese rind communities across the surfaces of cheese and variation in community composition across wheels of cheese [50, 54, 92]. Third, we only considered how one neighboring species at a time impacts the evolution of *S. xylosus* and did not consider how combinations of species drive phenotypic and genomic evolution of this bacterium. For example, combining *D. hansenii* with a neighbor that decreased the fitness of evolved strains might inhibit the global regulator evolution observed when only *D. hansenii* was present.

A major question that remains unanswered is why does *D. hansenii* promote the diversification of *S. xylosus* on cheese? We did not identify specific mechanisms underlying *Staphylococcus-Debaryomyces* interactions, but several lines of evidence from our data and the cheese rind system provide some helpful clues. One ecological explanation is that the degree of niche overlap between these two species may promote diversification of *S. xylosus*. A common theme in the study of adaptation to novel environments is that interspecific interactions can promote diversification when there is strong niche overlap [32]. *Staphylococcus* species and yeasts such as *D. hansenii* share similar resource and temporal niches in cheese rind microbiomes. At the early stages of cheese ripening, the pH of cheese is low, salt concentrations are high, and resources such as free amino acids are locked up in the casein of cheese. Previous work in our lab and others has shown that both *S. xylosus* and *D. hansenii* grow early in cheese succession [50, 54, 93]. These microbes are both tolerant of high salt concentrations and have proteolytic abilities that help them access free amino acids in cheese. In contrast, the other two biotic neighbors (*Brevibacterium* and *Penicillium*) grow later in cheese rind succession and occupy different niches compared to *Staphylococcus*. During our evolution experiment, competition for resources between *S. xylosus* and *D. hansenii* may have promoted the adaptation of new lineages of *S. xylosus* with different metabolic and ecological traits.

Another potential explanation for the abundance of evolved strains with altered global regulation is that these strains are only able to persist in the presence of *D. hansenii* due to facilitative interactions between the yeast and evolved strains. Both the ancestor and evolved *S. xylosus* strains had slightly higher growth in the presence of *D. hansenii*, suggesting that the yeast does provide some benefits for the bacterium. RNA-seq demonstrated strong metabolic downregulation of many pathways in evolved strains, including biosynthesis of histidine and other amino acids. *D. hansenii* may have promoted the rapid and reproducible rise of these strains through unknown mechanisms of supplementing their altered metabolism. For example, *D. hansenii* may break down some cheese curd components and release nutrients that are needed to support the altered metabolism of the *S. xylosus* with mutations in global regulators. Future work using metabolomics will help pinpoint the chemical mediators of *sigB*, *agr*, and *walRK* evolution in the *D. hansenii* environment.

Our evolution experiment demonstrates how interspecific interactions might facilitate the generation of strain diversity within microbiomes. These data also contribute to an emerging body of work demonstrating that microbes have very different evolutionary outcomes when biotic complexity is incorporated into experimental evolution [30, 33, 35, 36, 94, 95]. Because most medically and industrially important microbes often live with other microbial species that may impose strong biotic selection

[23, 25, 96, 97], the management and engineering of microbiomes may need to incorporate how microbe-microbe interactions can shape evolution. As additional studies use a broader range of target microbes and more diverse biotic environments, we can begin to create a predictive framework for when and how interspecific interactions can impact microbial evolution.

METHODS

Experimental evolution

All yeast and bacterial cultures were maintained as frozen stocks in 15% glycerol in a −80 °C freezer. The main target for experimental evolution, *S. xylosus* strain BC10, was originally isolated from the surface of a natural rind cheese made in Vermont, USA and has been previously described [50]. Three different microbial strains were used as neighbor treatments: *Brevibacterium aurantiacum* strain JB5 (as previously described in [53]), *Penicillium solitum* strain #12 (as previously described in [47]), and the yeast *D. hansenii* strain 135B (as previously described in [50]). All of these strains were isolated from one natural rind cheese made in the same aging facility and commonly co-occur in natural rind cheeses made in different regions of the world [50, 54, 98–100].

To initiate the evolution experiments, cultures were inoculated into 1.5 mL microcentrifuge tubes filled with a 150 µL aliquot of cheese curd agar (CCA) containing 3% salt (w/w) [101]. Inoculum for each culture came from frozen glycerol stocks where a known CFU/µL concentration of the microbial culture had been previously determined [101]. In the alone and +neighbor treatments, 50 CFUs of *S. xylosus* were inoculated into each replicate tube by adding 10 µL of inoculum suspended in 1X phosphate buffered saline (PBS) to the CCA surface. In each of the neighbor treatments, 50 CFUs of a neighbor were added to the *S. xylosus* inoculum. Each treatment was replicated 10 times. One replicate from the +*Debaryomyces* treatment was lost during the experiment due to contamination. Tubes were covered with sterile AeraSeal films and then placed in microcentrifuge tube racks containing a snack Ziplock bag with a paper towel moistened with 5 mL of sterile PBS to maintain high humidity. A lid was placed on the tube rack to contain the moisture and tubes were incubated in the dark for 7 days at 24 °C.

After 7 days of growth, each population was transferred by adding 300 µL of 15% glycerol to the existing population, homogenizing the sample with a micropestle, and pipetting 10 µL of the homogenate using a wide orifice pipette tip to a fresh 1.5 mL microcentrifuge tube containing 150 µL of CCA. Each homogenized sample was then frozen at −80 °C to serve as fossil stocks for isolating colonies. This was repeated over a period of 15 weeks.

To determine the frequency of mutant phenotypes within the population at each transfer, 20 µL of homogenate was serially diluted and plated onto plate count agar with milk and salt (PCAMS, [101]) plates with 50 mg/L of cycloheximide to inhibit the growth of fungi. Plates were incubated at 24 °C with natural room light to allow for the development of colony pigmentation. Plates were scored for mutant frequency by counting colonies and noting the presence of colonies with altered phenotypes. Wild-type *S. xylosus* BC10 is intensely orange/yellow in color, wrinkly, and shiny. Colonies deemed phenotypic mutants had abnormal pigmentation (white, light yellow), colony texture (less wrinkly to completely smooth), and colony surface appearance (matte or partially shiny). Abundances of neighbors were also determined by plating onto selective media for fungi (PCAMS + 50 mg/L of chloramphenicol to inhibit bacteria) or by counting colonies of *Brevibacterium* that grew alongside the *S. xylosus* colonies.

Whole-genome sequencing and analysis

To identify genomic changes in evolved isolates, whole-genome sequencing was conducted on seven randomly selected colonies from the final time point from three populations across the four treatments (84 genomes in total). DNA was extracted from streaks of pure cultures growing on PCAMS plates using a MoBio PowerSoil DNA Isolation kit. Sequencing libraries for each genome were constructed using the NEBNext Ultra DNA Library Prep Kit for Illumina (New England Biolabs) using the manufacturer's protocol with DNA input concentrations of 5–15 ng/µL, a 20-min fragmentase incubation for DNA fragmentation, and 5 rounds of PCR enrichment. Equimolar concentrations of each library representing isolate genomes were pooled and sequenced in one HiSeq 2500 run at the Harvard FAS Center for Systems Biology Core Facility. We aimed to have at least ~20–30X coverage of each genome for variant detection. Mean coverage across all libraries was 39.4.

Reads were mapped to a reference genome of *S. xylosus* BC10 (NCBI WGS Project LNPU00000000) using end-to-end alignment in Bowtie2 [102]. We also mapped reads of the ancestral isolate to the reference genome to identify any errors in the original genome assembly that could cause erroneous variant calling. Variant calling was conducted using FreeBayes in pooled continuous mode with the following settings: ploidy = 1, minimum alternate count = 10 (a coverage of at least 10 reads needed to support variant calls), minimum alternate fraction = 0.9 (at least 90% of mapped reads needed to contain the variant in order for it to be called), and minimum probability = 0.1. Any SNPs or other variants identified from mapping raw reads of the ancestor were excluded from variant calls of the evolved isolates. When read mapping indicated potential deletion or other structural variants, we re-assembled the genomes of those isolates using SPAdes and annotated the genome using RASTk.

Phenotypic assays

To measure staphyloxanthin production, bacteria were streaked across a PCAMS plate and were left to grow for one week to develop pigment. Each plate was laid out singly in a plastic bag to ensure each plate received even exposure to light. After one week of growth at 24 °C, 20 mg of cells were removed from the plate with a wooden dowel. Cells were resuspended in 800 µL of methanol and thoroughly mixed via vortexing. The suspensions were left overnight at 55 °C with shaking at 525 rpm on a benchtop shaking incubator to extract the pigment from cells. After extractions, the suspensions were centrifuged at 5000 g for 10 min. The pellets appeared colorless (white) with the pigment in the supernatant. The absorbance of the supernatant was read at 465 nm using methanol as a blank. The absorbance readings were normalized to cell weight.

To quantify biofilm production, bacteria were grown in 5 mL brain heart infusion (BHI) broth overnight at 24 °C. The cells were diluted 100-fold in BHI, and 200 µL of inoculum was added to eight wells of a flat-bottom 96-well plate (Falcon). After 16 h of growth at 24 °C, the OD_{600} was recorded to account for differential growth of each strain. Wells were washed three times by manually flipping plates to dispose of liquid and adding 200 µL of 1X PBS to the wells to remove dislodged cells. The cells were heat fixed to the plate by incubating for 1 h at 60 °C. Fifty microliters of a solution of 0.06% crystal violet stain was added to each sample. These were incubated for 5 min at room temperature and rinsed three times with 200 µL of 1× PBS. Biofilm formation was estimated by solubilization of crystal violet by adding 200 µL of 30% acetic acid and determining the OD_{600}. For each of three independent experiments, 8–12 replicate wells in three replicate plates were used.

The effect of mutations on bacterial spreading was assessed on soft BHI agar (0.4% w/v). After autoclaving, the medium was cooled down to 50 °C and 20 mL was poured into Petri dishes. The plates were kept at room temperature for 3 h prior to spreading assay. Bacterial strains were grown in 5 mL BHI broth overnight at room temperature. The cells were adjusted to OD_{600} of 1, and 2 µL of the cell suspension was spotted in the center of a 0.4% and 1.5% BHI agar plate. The plates were incubated for 5 days at 24 °C. Spreading diameter was calculated by measuring the largest diameter of the colony for each of five replicates.

To measure oxidative stress tolerance, inocula of BC10, 51_3, 51_7, 55_5, 60_1, 60_5 grown for 16 h in BHI broth were standardized to OD_{600} of 0.5 and incubated in 200 µL of different concentrations of H_2O_2 (0, 50, 100, 150, 200 mM) in the dark at 24 °C. After 45 min, the reaction was stopped with the addition of 2 U/mL catalase and incubation for 20 min. Cells were serially diluted and plated on PCAMS to quantify CFUs. Values are expressed as a percentage of the CFU in the control lacking H_2O_2 and are the averages of eight replicates in two independent experiments.

RNA sequencing

To characterize the transcriptomes of the ancestor and three evolved strains with mutant colony phenotypes (51_3, 55_5, and 60_1), we constructed and analyzed RNA-seq libraries. Lawns of each strain were grown on 100 mm Petri dishes containing 10% CCA media with 3% salt. Bacteria were inoculated at 50,000 CFUs and plates were incubated at 24 °C for 3 days. Bacterial cells were harvested from the surface of the CCA using a sterile razor blade and were then immediately placed into 3 mL of RNAProtect Bacteria Reagent (Qiagen) and frozen at −80 °C until RNA extraction. Total RNA was extracted as previously detailed using a 125:24:1 (v/v/v) phenol/chloroform/isoamyl alcohol extraction [55, 101]. Bacterial rRNA was depleted using a NEBNext Bacteria rRNA Depletion Kit, and depleted RNA was used to construct libraries using the NEBNext Ultra RNA Library Prep Kit for Illumina. Libraries were sequenced using a NextSeq 550 with single-end 75 base-pair reads. Reads were mapped to the *S. xylosus*

BC10 draft genome (GenBank Assembly Accession: GCA_001747745.1) using Bowtie2, and differentially expressed genes were identified using DESeq2 with a $\log_2$ ratio of 1/−1 and FDR corrected p value of <0.05. To identify pathways that were enriched in the differentially expressed genes, we used the Gene-List Enrichment tool of KOBAS [103] with our BC10 draft genome as the background genes to test for enrichment.

Growth and competition experiments

To determine the ability of the ancestor and evolved strains to grow on cheese, each was inoculated at a concentration of 667 CFUs onto the surface of 150 µL of CCA in a 1.5 mL Eppendorf tube. Experimental units were incubated as described for the evolution experiment above. Growth of cells over time was determined at 1, 2, 3, 4 and 7 days by resuspending the cells into 300 µL of 30% glycerol. The cells and CCA were homogenized via pestling, serially diluted, and plated onto PCAMS to determine CFUs. To determine how the yeast *D. hansenii* strain 135B impacted the short-term growth of the ancestor and evolved *S. xylosus* strains, the same experimental approach was used with 667 CFUs of *D. hansenii* added to the +*Debaryomyces* treatment.

To determine the fitness of mutant strains, we competed three evolved strains (51_3, 55_5, and 60_1) against the ancestor strain in 50:50 initial ratios either alone (with no neighbor) or in the three biotic treatments (+*Debaryomyces*, +*Brevibacterium*, +*Penicillium*). Each strain (*S. xylosus* BC10 ancestor, *S. xylosus* BC10 evolved strain, and *Debaryomyces/Brevibacterium/Penicillium* if present) was inoculated at a concentration of 667 CFUs into 1.5 mL Eppendorf tubes containing 150 µL of CCA. After one week of incubation at 24 °C under aerobic conditions, cells were harvested by resuspending the wells into 300 µL of 30% glycerol and homogenizing via pestling. Ten microliters of the homogenized communities were transferred to a new tube and were incubated for another week to mimic the multiple rounds of growth that are experienced in the experimental evolution design and to amplify small fitness differences that might be observed in only one round of growth. This was repeated for a total of five transfers. We acknowledge that some mutations may occur in the ancestor strains during the five transfers and that this could increase the observance of mutant colony phenotypes. However, this should happen relatively rarely based on the frequency of mutant colonies we observed in our original evolution experiment (Fig. 1D). To determine the abundance of ancestor and mutant colonies at each transfer, 20 µL of the homogenized sample was serially diluted and plated onto PCAMS. Mutant colonies could be distinguished from ancestor colonies due to their reduced pigmentation and altered colony morphology. This experiment continued for a total of five weeks. Relative fitness of the mutant strains was calculated as $\log_{10}((\text{CFUs of mutant strain} + 1) \div (\text{CFUs of ancestor strain} + 1))$. A second competition experiment was conducted to confirm the observed fitness patterns observed in the first experiment. It was executed using the same setup, transfer, and plating methods as above, but with only the Alone and +*Debaryomyces* treatments. This second experiment was conducted for only three weeks.

Statistics

To assess whether there were significant differences in the frequencies of phenotypic mutants or mutations across the experimental evolution populations (Figs. 1 and 2), we used ANOVA with Tukey's post-hoc tests. We also used ANOVAs with Dunnett's multiple comparison tests or Tukey's post-hoc tests to assess differences in the phenotypic assays (Fig. 3). To identify differentially expressed genes in the RNA-seq data (Fig. 4), DESeq2 was used with a significance cutoff of a $\log_2$ ratio of 1/−1 and a FDR corrected p value of <0.05. For RNA-seq pathway enrichment, we used Fisher's exact tests with Benjamini and Hochberg false discovery rate correction in the Gene-List Enrichment Tool of KOBAS. To determine if there were differences in growth of the strains over time (Fig. 5A), a repeated-measures ANOVA was used. To assess whether *D. hansenii* impacted the growth of *S. xylosus* BC10 ancestor and mutant strains (Fig. 5B), an ANOVA on the day 7 CFU data was used. To determine how biotic environments affected the fitness of ancestor and mutant BC10 strains (Fig. 5C), ANOVAs were used for each mutant strain. Log transformations were applied when appropriate. All statistical analyses were conducted in PRISM 9 or R.

DATA AVAILABILITY

All raw fastq read files of re-sequenced evolved isolates of *S. xylosus* BC10 have been deposited in NCBI in BioProject PRJNA856679. Raw RNA-seq read files from this study have been deposited in NCBI in BioProject PRJNA856810.

REFERENCES

1. Monk JM, Koza A, Campodonico MA, Machado D, Seoane JM, Palsson BO, et al. Multi-omics quantification of species variation of *Escherichia coli* links molecular features with strain phenotypes. Cell Syst. 2016;3:238–51.
2. McCloskey D, Xu J, Schrübbers L, Christensen HB, Herrgård MJ. RapidRIP quantifies the intracellular metabolome of 7 industrial strains of *E. coli*. Metab Eng. 2018;47:383–92.
3. Garay-Arroyo A, Covarrubias AA, Clark I, Niño I, Gosset G, Martinez A. Response to different environmental stress conditions of industrial and laboratory *Saccharomyces cerevisiae strains*. Appl Microbiol Biotechnol. 2004;63:734–41.
4. Gallone B, Steensels J, Prahl T, Soriaga L, Saels V, Herrera-Malaver B, et al. Domestication and divergence of *Saccharomyces cerevisiae* beer yeasts. Cell. 2016;166:1397–410.
5. Des Roches S, Post DM, Turley NE, Bailey JK, Hendry AP, Kinnison MT, et al. The ecological importance of intraspecific variation. Nat Ecol Evol. 2018;2:57–64.
6. Leventhal GE, Boix C, Kuechler U, Enke TN, Sliwerska E, Holliger C, et al. Strain-level diversity drives alternative community types in millimetre-scale granular biofilms. Nat Microbiol. 2018;3:1295–303.
7. Ellegaard KM, Engel P. Beyond 16S rRNA community profiling: intra-species diversity in the gut microbiota. Front Microbiol. 2016;7:1475.
8. Warringer J, Zörgö E, Cubillos FA, Zia A, Gjuvsland A, Simpson JT, et al. Trait variation in yeast is defined by population history. PLoS Genet. 2011;7:e1002111.
9. Steensels J, Snoek T, Meersman E, Picca Nicolino M, Voordeckers K, Verstrepen KJ. Improving industrial yeast strains: exploiting natural and artificial diversity. FEMS Microbiol Rev. 2014;38:947–95.
10. Van Rossum T, Ferretti P, Maistrenko OM, Bork P. Diversity within species: interpreting strains in microbiomes. Nat Rev Microbiol. 2020;18:491–506.
11. Lenski RE. Experimental evolution and the dynamics of adaptation and genome evolution in microbial populations. ISME J. 2017;11:2181–94.
12. Elena SF, Lenski RE. Microbial genetics: evolution experiments with microorganisms: the dynamics and genetic bases of adaptation. Nat Rev Genet. 2003;4:457.
13. Cooper VS. Experimental evolution as a high-throughput screen for genetic adaptations. mSphere. 2018;3:e00121–18.
14. Long A, Liti G, Luptak A, Tenaillon O. Elucidating the molecular architecture of adaptation via evolve and resequence experiments. Nat Rev Genet. 2015;16:567–82.
15. Kassen R. Experimental evolution of innovation and novelty. Trends Ecol Evol. 2019;34:712–22.
16. Kawecki TJ, Lenski RE, Ebert D, Hollis B, Olivieri I, Whitlock MC. Experimental evolution. Trends Ecol Evol. 2012;27:547–60.
17. Kassen R. Experimental evolution and the nature of biodiversity. Greenwood Village, CO: Roberts & Company; 2014.
18. Bailey SF, Bataillon T. Can the experimental evolution programme help us elucidate the genetic basis of adaptation in nature? Mol Ecol. 2016;25:203–18.
19. Jessup CM, Kassen R, Forde SE, Kerr B, Buckling A, Rainey PB, et al. Big questions, small worlds: microbial model systems in ecology. Trends Ecol Evol. 2004;19:189–97.
20. Hibbing ME, Fuqua C, Parsek MR, Peterson SB. Bacterial competition: surviving and thriving in the microbial jungle. Nat Rev Microbiol. 2010;8:15–25.
21. Little AEF, Robinson CJ, Peterson SB, Raffa KF, Handelsman J. Rules of engagement: interspecies interactions that regulate microbial communities. Annu Rev Microbiol. 2008;62:375–401.
22. Frey-Klett P, Burlinson P, Deveau A, Barret M, Tarkka M, Sarniguet A. Bacterial-fungal interactions: hyphens between agricultural, clinical, environmental, and food microbiologists. Microbiol Mol Biol Rev. 2011;75:583–609.
23. Deveau A, Bonito G, Uehling J, Paoletti M, Becker M, Bindschedler S, et al. Bacterial–fungal interactions: ecology, mechanisms and challenges. FEMS Microbiol Rev. 2018;42:335–52.
24. Pacheco AR, Segrè D. A multidimensional perspective on microbial interactions. FEMS Microbiol Lett. 2019;366:fnz125.
25. Cosetta CM, Wolfe BE. Causes and consequences of biotic interactions within microbiomes. Curr Opin Microbiol. 2019;50:35–41.
26. Johansson J. Evolutionary responses to environmental changes: how does competition affect adaptation? Evolution. 2008;62:421–35.
27. Stuart YE, Campbell TS, Hohenlohe PA, Reynolds RG, Revell LJ, Losos JB. Rapid evolution of a native species following invasion by a congener. Science. 2014;346:463–6.
28. Zhang Q-G, Ellis RJ, Godfray HCJ. The effect of a competitor on a model adaptive radiation. Evolution. 2012;66:1985–90.
29. Harcombe W. Novel cooperation experimentally evolved between species. Evolution. 2010;64:2166–72.
30. Lawrence D, Fiegna F, Behrends V, Bundy JG, Phillimore AB, Bell T, et al. Species interactions alter evolutionary responses to a novel environment. PLoS Biol. 2012;10:e1001330.

31. Lahti DC, Johnson NA, Ajie BC, Otto SP, Hendry AP, Blumstein DT, et al. Relaxed selection in the wild. Trends Ecol Evol. 2009;24:487–96.
32. Bailey SF, Dettman JR, Rainey PB, Kassen R. Competition both drives and impedes diversification in a model adaptive radiation. Proc Biol Sci. 2013;280:20131253.
33. Hall JPJ, Harrison E, Brockhurst MA. Competitive species interactions constrain abiotic adaptation in a bacterial soil community. Evol Lett. 2018;2:580–9.
34. Jousset A, Eisenhauer N, Merker M, Mouquet N, Scheu S. High functional diversity stimulates diversification in experimental microbial communities. Sci Adv. 2016;2:e1600124.
35. Scheuerl T, Hopkins M, Nowell RW, Rivett DW, Barraclough TG, Bell T. Bacterial adaptation is constrained in complex communities. Nat Commun. 2020;11:754.
36. Golzar FS, Ferguson GC, Hendrickson HL. Protozoan predation drives adaptive divergence in *Pseudomonas fluorescens* SBW25; ecology meets experimental evolution. *bioRxiv*. 2021. https://doi.org/10.1101/2021.07.12.452127.
37. Chu X-L, Zhang Q-G, Buckling A, Castledine M. Interspecific niche competition increases morphological diversity in multi-species microbial communities. Front Microbiol. 2021;12:2103.
38. Wolfe BE, Dutton RJ. Fermented foods as experimentally tractable microbial ecosystems. Cell. 2015;161:49–55.
39. Di Cagno R, Coda R, De Angelis M, Gobbetti M. Exploitation of vegetables and fruits through lactic acid fermentation. Food Microbiol. 2013;33:1–10.
40. De Vuyst L, Van Kerrebroeck S, Harth H, Huys G, Daniel H-M, Weckx S. Microbial ecology of sourdough fermentations: diverse or uniform? Food Microbiol. 2014;37:11–29.
41. Montel M-C, Buchin S, Mallet A, Delbes-Paus C, Vuitton DA, Desmasures N, et al. Traditional cheeses: rich and diverse microbiota with associated benefits. Int J Food Microbiol. 2014;177:136–54.
42. Macori G, Cotter PD. Novel insights into the microbiology of fermented dairy foods. Curr Opin Biotechnol. 2018;49:172–8.
43. Steensels J, Gallone B, Voordeckers K, Verstrepen KJ. Domestication of industrial microbes. Curr Biol. 2019;29:R381–R393.
44. Gibbons JG, Rinker DC. The genomics of microbial domestication in the fermented food environment. Curr Opin Genet Dev. 2015;35:1–8.
45. Gibbons JG, Salichos L, Slot JC, Rinker DC, McGary KL, King JG, et al. The evolutionary imprint of domestication on genome variation and function of the filamentous fungus *Aspergillus oryzae*. Curr Biol. 2012;22:1403–9.
46. Ropars J, Rodríguez de la Vega RC, López-Villavicencio M, Gouzy J, Sallet E, Dumas É, et al. Adaptive horizontal gene transfers between multiple cheese-associated fungi. Curr Biol. 2015;25:2562–9.
47. Bodinaku I, Shaffer J, Connors AB, Steenwyk JL, Kastman E, Rokas A, et al. Rapid phenotypic and metabolomic domestication of wild *Penicillium* molds on cheese. mBio. 2019;10:e02445–19.
48. Heo S, Lee J-H, Jeong D-W. Food-derived coagulase-negative *Staphylococcus* as starter cultures for fermented foods. Food Sci Biotechnol. 2020;29:1023–35.
49. Nagase N, Sasaki A, Yamashita K, Shimizu A, Wakita Y, Kitai S, et al. Isolation and species distribution of staphylococci from animal and human skin. J Vet Med Sci. 2002;64:245–50.
50. Kastman EK, Kamelamela N, Norville JW, Cosetta CM, Dutton RJ, Wolfe BE. Biotic interactions shape the ecological distributions of *Staphylococcus* Species. mBio. 2016;7:e01157–16.
51. Savage VJ, Chopra I, O'Neill AJ. Population diversification in *Staphylococcus aureus* biofilms may promote dissemination and persistence. PLoS ONE. 2013;8:e62513.
52. Koch G, Yepes A, Förstner KU, Wermser C, Stengel ST, Modamio J, et al. Evolution of resistance to a last-resort antibiotic in *Staphylococcus aureus* via bacterial competition. Cell. 2014;158:1060–71.
53. Niccum BA, Kastman EK, Kfoury N, Robbat A Jr, Wolfe BE. Strain-level diversity impacts cheese rind microbiome assembly and function. mSystems. 2020;5:e00149–20.
54. Wolfe BE, Button JE, Santarelli M, Dutton RJ. Cheese rind communities provide tractable systems for in situ and in vitro studies of microbial diversity. Cell. 2014;158:422–33.
55. Cosetta CM, Kfoury N, Robbat A, Wolfe BE. Fungal volatiles mediate cheese rind microbiome assembly. Environ Microbiol. 2020;22:4745–60.
56. Hu G, Wang Y, Liu X, Strube ML, Wang B, Kovács ÁT. Species and condition dependent mutational spectrum in experimentally evolved biofilms of Bacilli. *bioRxiv*. 2022. https://doi.org/10.1101/2022.12.07.519423.
57. Lanfear R, Kokko H, Eyre-Walker A. Population size and the rate of evolution. Trends Ecol Evol. 2014;29:33–41.
58. Zhao X-F, Buckling A, Zhang Q-G, Hesse E. Specific adaptation to strong competitors can offset the negative effects of population size reductions. Proc Biol Sci. 2018;285:2018000.
59. Schaik A. The role of σB in the stress response of Gram-positive bacteria–targets for food preservation and safety. Curr Opin Biotechnol. 2005;16:218–24.
60. Bischoff M, Entenza JM, Giachino P. Influence of a functional *sigB* operon on the global regulators *sar* and *agr* in *Staphylococcus aureus*. J Bacteriol. 2001;183:5171–9.
61. Guldimann C, Boor KJ, Wiedmann M, Guariglia-Oropeza V. Resilience in the face of uncertainty: sigma factor B fine-tunes gene expression to support homeostasis in gram-positive bacteria. Appl Environ Microbiol. 2016;82:4456–69.
62. Robinson DA, Monk AB, Cooper JE, Feil EJ, Enright MC. Evolutionary genetics of the accessory gene regulator (*agr*) locus in *Staphylococcus aureus*. J Bacteriol. 2005;187:8312–21.
63. Painter KL, Krishna A, Wigneshweraraj S, Edwards AM. What role does the quorum-sensing accessory gene regulator system play during *Staphylococcus aureus* bacteremia? Trends Microbiol. 2014;22:676–85.
64. Novick RP, Geisinger E. Quorum sensing in staphylococci. Annu Rev Genet. 2008;42:541–64.
65. Martin PK, Li T, Sun D, Biek DP, Schmid MB. Role in cell permeability of an essential two-component system in *Staphylococcus aureus*. J Bacteriol. 1999;181:3666–73.
66. Ji Q, Chen PJ, Qin G, Deng X, Hao Z, Wawrzak Z, et al. Structure and mechanism of the essential two-component signal-transduction system WalKR in *Staphylococcus aureus*. Nat Commun. 2016;7:11000.
67. Dufour P, Jarraud S, Vandenesch F, Greenland T, Novick RP, Bes M, et al. High genetic variability of the *agr* locus in *Staphylococcus* species. J Bacteriol. 2002;184:1180–6.
68. Wuster A, Babu MM. Conservation and evolutionary dynamics of the *agr* cell-to-cell communication system across firmicutes. J Bacteriol. 2008;190:743–6.
69. Ferreira A, Gray M, Wiedmann M, Boor KJ. Comparative genomic analysis of the *sigB* operon in *Listeria monocytogenes* and in other Gram-positive bacteria. Curr Microbiol. 2004;48:39–46.
70. Xue L, Chen YY, Yan Z, Lu W, Wan D, Zhu H. Staphyloxanthin: a potential target for antivirulence therapy. Infect Drug Resist. 2019;12:2151–60.
71. Marbach H, Mayer K, Vogl C, Lee JYH, Monk IR, Sordelli DO, et al. Within-host evolution of bovine *Staphylococcus aureus* selects for a SigB-deficient pathotype characterized by reduced virulence but enhanced proteolytic activity and biofilm formation. Sci Rep. 2019;9:13479.
72. Clauditz A, Resch A, Wieland K-P, Peschel A, Götz F. Staphyloxanthin plays a role in the fitness of *Staphylococcus aureus* and its ability to cope with oxidative stress. Infect Immun. 2006;74:4950–3.
73. Liu GY, Essex A, Buchanan JT, Datta V, Hoffman HM, Bastian JF, et al. *Staphylococcus aureus* golden pigment impairs neutrophil killing and promotes virulence through its antioxidant activity. J Exp Med. 2005;202:209–15.
74. Davey ME, O'toole GA. Microbial biofilms: from ecology to molecular genetics. Microbiol Mol Biol Rev. 2000;64:847–67.
75. Flemming H-C, Wingender J, Szewzyk U, Steinberg P, Rice SA, Kjelleberg S. Biofilms: an emergent form of bacterial life. Nat Rev Microbiol. 2016;14:563–75.
76. Moons P, Michiels CW, Aertsen A. Bacterial interactions in biofilms. Crit Rev Microbiol. 2009;35:157–68.
77. Bateman BT, Donegan NP, Jarry TM, Palma M, Cheung AL. Evaluation of a tetracycline-inducible promoter in *Staphylococcus aureus* in vitro and in vivo and its application in demonstrating the role of sigB in microcolony formation. Infect Immun. 2001;69:7851–7.
78. Lauderdale KJ, Boles BR, Cheung AL, Horswill AR. Interconnections between Sigma B, agr, and proteolytic activity in *Staphylococcus aureus* biofilm maturation. Infect Immun. 2009;77:1623–35.
79. Vuong C, Saenz HL, Götz F, Otto M. Impact of the agr quorum-sensing system on adherence to polystyrene in *Staphylococcus aureus*. J Infect Dis. 2000;182:1688–93.
80. Pollitt EJG, Crusz SA, Diggle SP. *Staphylococcus aureus* forms spreading dendrites that have characteristics of active motility. Sci Rep. 2015;5:17698.
81. Pollitt EJG, Diggle SP. Defining motility in the Staphylococci. Cell Mol Life Sci. 2017;74:2943–58.
82. Kaito C, Sekimizu K. Colony spreading in *Staphylococcus aureus*. J Bacteriol. 2007;189:2553–7.
83. Dordet-Frisoni E, Gaillard-Martinie B, Talon R, Leroy S. Surface migration of *Staphylococcus xylosus* on low-agar media. Res Microbiol. 2008;159:263–9.
84. Tsompanidou E, Denham EL, Becher D, de Jong A, Buist G, van Oosten M, et al. Distinct roles of phenol-soluble modulins in spreading of *Staphylococcus aureus* on wet surfaces. Appl Environ Microbiol. 2013;79:886–95.
85. Xu T, Wang X-Y, Cui P, Zhang Y-M, Zhang W-H, Zhang Y. The agr quorum sensing system represses persister formation through regulation of phenol soluble modulins in *Staphylococcus aureus*. Front Microbiol. 2017;8:2189.
86. Aubourg M, Pottier M, Léon A, Bernay B, Dhalluin A, Cacaci M, et al. Inactivation of the response regulator AgrA has a pleiotropic effect on biofilm formation, pathogenesis and stress response in *Staphylococcus lugdunensis*. Microbiol Spectr. 2022;10:e0159821.
87. Rao Y, Peng H, Shang W, Hu Z, Yang Y, Tan L, et al. A vancomycin resistance-associated WalK(S221P) mutation attenuates the virulence of vancomycin-intermediate *Staphylococcus aureus*. J Adv Res. 2021;40:167–78.

88. Altman DR, Sullivan MJ, Chacko KI, Balasubramanian D, Pak TR, Sause WE, et al. Genome plasticity of *agr*-defective *Staphylococcus aureus* during clinical infection. Infect Immun. 2018;86:e00331–18.
89. Shoji M, Cui L, Iizuka R, Komoto A, Neoh H-M, Watanabe Y, et al. walK and clpP mutations confer reduced vancomycin susceptibility in *Staphylococcus aureus*. Antimicrob Agents Chemother. 2011;55:3870–81.
90. Leroy S, Even S, Micheau P, de La Foye A, Laroute V, Le Loir Y, et al. Transcriptomic analysis of *Staphylococcus xylosus* in solid dairy matrix reveals an aerobic lifestyle adapted to rind. Microorganisms. 2020;8:1807.
91. Chen P, Zhang J. Antagonistic pleiotropy conceals molecular adaptations in changing environments. Nat Ecol Evol. 2020;4:461–9.
92. Quigley L, O'Sullivan O, Beresford TP, Paul Ross R, Fitzgerald GF, Cotter PD. High-throughput sequencing detects subpopulations of bacteria not previously associated with artisanal cheeses. Appl Environ Microbiol. 2012;78:5717–23.
93. Mounier J, Monnet C, Vallaeys T, Arditi R, Sarthou A-S, Hélias A, et al. Microbial interactions within a cheese microbial community. Appl Environ Microbiol. 2008;74:172–81.
94. Barber JN, Nicholson LC, Woods LC, Judd LM, Sezmis AL, Hawkey J, et al. Species interactions constrain adaptation and preserve ecological stability in an experimental microbial community. ISME J. 2022;16:1442–52.
95. Gómez P, Hall AR, Paterson S, Buckling A. Rapid decline of adaptation of *Pseudomonas fluorescens* to soil biotic environment. Biol Lett. 2022;18:20210593.
96. Peleg AY, Hogan DA, Mylonakis E. Medically important bacterial–fungal interactions. Nat Rev Microbiol. 2010;8:340–9.
97. Pierce EC, Dutton RJ. Putting microbial interactions back into community contexts. Curr Opin Microbiol. 2022;65:56–63.
98. Addis E, Fleet GH, Cox JM, Kolak D, Leung T. The growth, properties and interactions of yeasts and bacteria associated with the maturation of Camembert and blue-veined cheeses. Int J Food Microbiol. 2001;69:25–36.
99. Bertuzzi AS, Walsh AM, Sheehan JJ, Cotter PD, Crispie F, McSweeney PLH, et al. Omics-based insights into flavor development and microbial succession within surface-ripened cheese. mSystems. 2018;3:e00211–17.
100. Larpin-Laborde S, Imran M, Bonaïti C, Bora N, Gelsomino R, Goerges S, et al. Surface microbial consortia from Livarot, a French smear-ripened cheese. Can J Microbiol. 2011;57:651–60.
101. Cosetta CM, Wolfe BE. Deconstructing and reconstructing cheese rind microbiomes for experiments in microbial ecology and evolution. Curr Protoc Microbiol. 2020;56:e95.
102. Langmead B, Salzberg SL. Fast gapped-read alignment with Bowtie 2. Nat Methods. 2012;9:357–9.
103. Bu D, Luo H, Huo P, Wang Z, Zhang S, He Z, et al. KOBAS-i: intelligent prioritization and exploratory visualization of biological functions for gene enrichment analysis. Nucleic Acids Res. 2021;49:W317–W325.

ACKNOWLEDGEMENTS

This work was funded by a grant from the United States National Science Foundation (CAREER IOS/BIO 1942063) to BEW. The authors are grateful to members of the Wolfe lab, including Robert May, Nicolas Louw, Kasturi Lele, Dillon Arrigan, Chris Tomo, and Mak Boylan, for providing extensive feedback on previous versions of this manuscript.

AUTHOR CONTRIBUTIONS

BN, CC, and BEW designed the study. BN conducted the evolution experiment. CC and BEW conducted the whole-genome resequencing. CC conducted the fitness experiments. BEW conducted and analyzed the RNA-seq experiment. CC, NK, MD, and MP conducted the phenotypic assays. CC, BN, and BEW conducted statistical analyses, created figures, and wrote the first drafts of the manuscript. All authors read, revised, and approved the final manuscript.

COMPETING INTERESTS

The authors declare no competing interests.

ADDITIONAL INFORMATION

Supplementary information The online version contains supplementary material available at https://doi.org/10.1038/s41396-023-01462-5.

Correspondence and requests for materials should be addressed to Benjamin E. Wolfe.